Theoret. Appl. Mech., Vol.35, No.1-3, pp. 73–91, Belgrade 2008

Dynamic interaction of cracks in piezoelectric and anisotropic solids: a non-hypersingular BIEM approach

Petia Dineva * **Dietmar Gross** †
Tsviatko Rangelov ‡

Abstract

A non-hypersingular traction *boundary integral equation method* (BIEM) is proposed for the treatment of crack systems in piezoelectric or anisotropic plane domains loaded by time-harmonic waves. The solution is based on the frequency dependent fundamental solution obtained by Radon transform. The proposed method is flexible, numerically efficient and has virtually no limitations regarding the material type, crack geometry and type of wave loading.

The accuracy and convergence of the BIEM solution for stress intensity factors is validated by comparison with existing results from the literature. Simulations for different crack configurations such as coplanar, collinear or cracks in arbitrary position to each other are presented and discussed. They demonstrate among others the strong effect of electromechanical coupling, show the frequency dependent shielding and amplification resulting from crack interaction and reveal the sensitivity of the K-factors on the complex influence of both wave-crack and crack-crack interaction.

Keywords: Piezoelectric or anisotropic material; wave scattering by multiple cracks; non-hypersingular traction BIEM; stress intensity factor.

*Department of Continuum Mechanics, Institute of Mechanics, Bulgarian Academy of Sciences, 1113 Sofia, Bulgaria

†Division of Solid Mechanics, Darmstadt University of Technology, 64289 Darmstadt, Germany

‡Department of Mathematical Physics, Institute of Mathematics and Informatics, Bulgarian Academy of Sciences, 1113 Sofia, Bulgaria

1 Introduction

Due to their coupled electro-mechanical behaviour piezoelectric materials and components are widely used in smart systems. At the same time their brittleness and low toughness make them very sensitive against defects like cracks or other stress concentrators. Therefore, static and dynamic crack analysis plays an important role though investigations are involved on account of the electro-mechanical coupling and the anisotropic nature of the material. While in the past mostly single cracks were in the focus of interest, the behaviour of multiple cracks, i.e. crack interaction, recently attracted increasing attention. One reason for that is the observation that a precursor of final failure often is the formation of interacting micro cracks which subsequently coalesce to a macro crack.

Crack systems under static loading have been studied by several authors. Without claiming completeness we mention Zhou and Wang [1], Sun [2] and Zhou *et* al. [3] who studied a symmetric system of parallel permeable cracks under anti-plane shear loading by pairs of triple integral equations. Closed-form solutions for the in-plane problem of collinear permeable cracks have been presented by Gao and Fan [4] who used the complex potential method while Han and Chen [5] considered parallel impermeable cracks. Zhou and Wu [6] solved the in-plane problem of two and of four parallel permeable cracks in an infinite region by dual integral equations. The results for the stress intensity factors (SIFs) show not only the amplification and shielding effects as they are known from classical isotropic materials but also the influence of the material parameters. They underline the strong effect of the electric crack interaction.

Less attention, compared with static loading, has been paid to crack systems under dynamic load, transient or time-harmonic. This refers to piezoelectric as well as to (uncoupled) anisotropic solids. It was Itou [7] and Itou and Haliding [8] who first computed SIFs for collinear and coplanar in-plane cracks in an infinite orthotropic plane subjected to time-harmonic plane wave by the method of dual integral equations.

A comprehensive treatment of the interaction between two cracks in a piezoelectric plane under steady state in-plane electrical and anti-plane mechanical loads is provided in Wang and Meguid [9-10]. Their analysis is based on singular integral equations coupled with a so-called pseudo-incident wave method; see Wang and Meguid [11]. With the same method Wang [12] solved the wave scattering of multiple permeable cracks in the interface between two infinite piezoelectric media. A similar problem was solved by Zhao and Meguid [13]. Meguid and Chen [14] studied the transient response of a finite piezoelectric strip with coplanar impermeable anti-plane cracks under electro-mechanical impact. Huang *et* al. [15] analysed the dynamic interaction among permeable

multiple cracks in a strip under anti-plane shear waves. The transient response of two coplanar cracks in a piezoelectric region under anti-plane mechanical and in-plane electric impact loads is investigated in Chen [16] and Chen and Worswick [17]. As further works shall be mentioned those of Sun *et* al. [18] on unequal parallel permeable interface cracks in a layer bonded to two piezoelectric half planes, Li and Lee [19] on two surface cracks and Su *et* al. [20] on coplanar interface cracks between two dissimilar piezoelectric strips. All these papers use the singular integral equation method and they are restricted to anti-plane problems and relatively simple crack and loading geometries.

Sanchez [21], Sanchez *et* al. [22] and Saez *et* al. [23] recently presented results for more involved in-plane problems of cracks in a piezoelectric or uncoupled anisotropic plane subjected to incident plane waves. In these works the hypersingular mixed (dual) BIEM formulation is developed, validated and applied where the displacement BIE is used over one of the crack surfaces while the hypersingular traction BIE is applied over the other crack surface. The treatment of the hypersingular integrals is carried out by means of variable change that transforms the boundary to the complex plane in conjunction with the singularity subtraction method.

The aim of the present paper is threefold. First, as an alternative to the just mentioned hypersingular mixed BIEM formulation the use of non-hypersingular traction BIEM for the treatment of crack systems shall be discussed. This method initially was introduced for the solution of wave scattering problems in isotropic cracked domains by Zhang and Gross [24] and later extended to single cracks in uncoupled anisotropic and piezoelectric media by Gross *et* al. [25] and Dineva *et* al. [26]. In this method the unknown variables are the displacement jumps across the crack faces. Its advantages are among others that all integrals are non-hypersingular and that discretization and collocation is necessary only along one of the crack's surfaces. Secondly, the flexibility, efficiency and accuracy of the method shall be demonstrated. These properties rely on the fundamental solution which is obtained by Radon transform and evaluated semi-analytically. By this means an anisotropic material may be considered as a simplified case of a piezoelectric material which needs no specific treatment. Finally, as examples of crack systems, various configurations of interacting in-plane cracks loaded by plane waves of different incident angles are considered. Parametric studies for the SIFs reveal the influence of the crack geometry, the incident wave's frequency and angle.

The paper is organized as follows. In section 2 the boundary-value-problem is formulated. The non-hypersingular traction based BIEM and its numerical realization are discussed in sections 3 and 4. Finally, in section 5, numerical examples are solved and validation and parametric studies are presented followed by some conclusions in section 6.

2 Problem statement

Consider an infinite, transversely isotropic piezoelectric domain containing N straight cracks $\Gamma_k, \quad k = 1, .., N$ of length $2a_k$ subjected to incident time-harmonic L- or SV- waves with angular frequency ω and incident angle θ with respect to x_1, see Figure 1. The material symmetry axis, i.e. the poling direction coincides with the x_3-axis and plane strain deformation is assumed in the x_1, x_3-plane. The non-zero field quantities then are the displacement u_i, the stress σ_{ij}, the dielectric displacement D_i and the electric field E_i, where $i, j = 1, 3$. The location of the $k-th$ crack with respect to the global x_1, x_3-

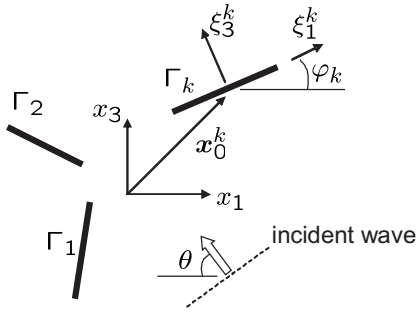

Figure 1: Crack system under harmonic wave loading

coordinate system can be described by the position vector (x_{01}^k, x_{03}^k) of the crack centre and the crack angle φ_k. With the local coordinates (ξ_1^k, ξ_3^k) and the accompanying unit vectors n^k, e^k, the points along the cracks are given by the position vector

$$x_i^k = x_{i0}^k + \xi_1^k e_i^k \quad , \quad \left|\xi_1^k\right| \leqslant a_k \quad . \tag{1}$$

The scattering problem in absence of volume forces and charges is described by the mechanical and electrical balance equations

$$\sigma_{ij,j} + \rho\omega^2 u_i = 0, \quad D_{j,j} = 0, \tag{2}$$

the strain-displacement and electric field-potential relations

$$s_{ij} = \frac{1}{2}\left(u_{i,j} + u_{j,i}\right) \quad E_i = -\Phi_{,i} \tag{3}$$

and the constitutive equations

$$\begin{array}{ll} \sigma_{11} = c_{11}u_{1,1} + c_{13}u_{3,3} + e_{31}\Phi_{,1} & D_1 = e_{15}u_{1,3} + e_{15}u_{3,1} - \varepsilon_{11}\Phi_{,1} \\ \sigma_{33} = c_{13}u_{1,1} + c_{33}u_{3,3} + e_{33}\Phi_{,3} & D_3 = e_{31}u_{1,1} + e_{33}u_{3,3} - \varepsilon_{33}\Phi_{,3} \\ \sigma_{13} = c_{44}u_{1,3} + c_{44}u_{3,1} + e_{15}\Phi_{,3} & \end{array} \tag{4}$$

Here Φ, s_{ij} and ρ are the electric potential, the strain tensor and the mass density, respectively. Subscript commas denote partial differentives and the summation convention over repeated indices is invoked. The material parameters consist on the elastic stiffnesses c_{11}, c_{33}, c_{44}, c_{13}, the dielectric constants ε_{11}, ε_{33} and the piezoelectric constants e_{31}, e_{33}, e_{15}. The problem statement is completed by the boundary condition along the crack faces and Sommerfeld's radiation condition at infinity. The crack faces, for simplicity, are assumed to be free of mechanical tractions and surface charges, i.e. impermeable cracks are assumed:

$$t_i = \sigma_{ij} n_j = 0, \quad D_j n_j = 0 \quad on \quad \Gamma = \bigcup_1^N \Gamma_k \tag{5}$$

Using the Davi and Milazzo [27] notation where $u_K = (u_1, u_3, \Phi)$, $s_{Kl} = (s_{11}, s_{33}, s_{13}, E_1, E_3)$, $\sigma_{iJ} = (\sigma_{11}, \sigma_{33}, \sigma_{13}, D_1, D_3)$, and $t_J = \sigma_{iJ} n_j$ are the generalized displacement, strain, stress and traction, respectively, equations (2), (3) and (4) can be written in the compact form

$$L(u) \equiv \sigma_{iJ,i} + \rho_{JK}\omega^2 u_K = 0 \quad with \quad \rho_{JK} = \begin{cases} \rho\ , & J\ , K = 1,3 \\ 0 & J = 4 \ or \ K\ = 4 \end{cases} \tag{6}$$

$$\sigma_{iJ} = C_{iJKl} u_{K,l} = C_{iJKl} s_{Kl} \tag{7}$$

where

$$C_{iJKl} = \begin{bmatrix} C & e \\ e' & -\varepsilon \end{bmatrix}, \quad C = \begin{bmatrix} c_{11} & c_{13} & 0 \\ c_{13} & c_{33} & 0 \\ 0 & 0 & c_{44} \end{bmatrix},$$

$$e = \begin{bmatrix} 0 & e_{31} \\ 0 & e_{33} \\ e_{15} & 0 \end{bmatrix}, \quad \varepsilon = \begin{bmatrix} \varepsilon_{11} & 0 \\ 0 & \varepsilon_{33} \end{bmatrix} \tag{8}$$

is the generalized stiffness tensor. The boundary condition (5) takes the form

$$t_J = 0 \quad on \quad \Gamma = \bigcup_1^N \Gamma_k \tag{9}$$

In the special case when the piezoelectric constants vanish, i.e. $e_{ij} = 0$, equations (6-9) degenerate to the uncoupled anisotropic case. As further specialization the mechanical isotropic case will be described when the stiffnesses are chosen as $C_{ijkl} = \lambda\delta_{ij}\delta_{kl} + \mu(\delta_{ik}\delta_{jl} + \delta_{il}\delta_{jk})$.

The total wave field can be written as a sum of the incident and the scattered wave field

$$u_J(x,\omega) = u_J^{in}(x,\omega) + u_J^{sc}(x,\omega), \quad t_J(x,\omega) = t_J^{in}(x,\omega) + t_J^{sc}(x,\omega) \tag{10}$$

where u_J^{in}, t_J^{in} and u_J^{sc}, t_J^{sc} are the incident and scattered generalized displacements and tractions, respectively, while $x = (x_1, x_3)$. The incident wave is prescribed as a plane time-harmonic P or SV wave. Its generalized displacement u_J^{in} and traction t_J^{in} are given in [25] for piezoelectric materials and in [26] for the anisotropic case. The scattered wave field is unknown and has to be determined. It has to satisfy equations (6-9), Sommerfeld's radiation condition at infinity and the boundary conditions (9) which in conjunction with (10) can be rewritten as

$$t_J^{sc} = -t_J^{in} \quad on \quad \Gamma_k, \quad k = 1, ...N \tag{11}$$

3 Non-hypersingular traction BIEM and numerical realization

Comparing the piezoelectric crack boundary value problem in generalized notation with that of the corresponding elastic problem, a total agreement can be stated. In view of this, following Gross and Zhang [28] and Zhang and Gross [24], the representation formula for the scattered wave field can be expressed as

$$u_J^{sc}(x,\omega) = -\sum_{k=1}^{N} \int\limits_{\Gamma_k} \sigma^*_{iMJ}(x,y,\omega)\Delta u_M^k(y,\omega) n_i^k(y) d\Gamma_k \ , \ x \notin \Gamma_k \tag{12}$$

where $x = (x_1, x_3)$ is the source point, $y = (y_1, y_3)$ is the observation point, $\sigma^*_{iJQ} = C_{iJKl} U^*_{KQ,l}$ is the stress derived from the fundamental solution U^*_{QK} of eq. (6). Its behavior including the spatial derivatives and asymptotic expansion for small arguments are discussed in [25] for piezoelectric materials and in [26] for the elastic anisotropic case. Furthermore, $\Delta u_J^k = u_J^k\big|_{\Gamma_k +} - u_J^k\big|_{\Gamma_k -}$ is the unknown generalized crack opening displacement (COD) on the crack Γ_k and n_i^k is the outward normal vector at the observation point on the $k-th$ crack Γ_k. The non-hypersingular traction boundary integral equation is obtained by differentiating (12), substituting the result into (6), satisfying the boundary condition (11) and taking the limit $x \to \Gamma_k$:

$$\begin{aligned} t_J^{in}(x,\omega) = C_{iJKl} n_i(x) \sum_{k=1}^{N} \int\limits_{\Gamma_k} \big[\big(\sigma^*_{\eta PK}(x,y,\omega)\Delta u^k_{P,\eta}(y,\omega) - \\ \rho_{QP}\omega^2 U^*_{QK}(x,y,\omega)\Delta u_P^k \delta_{\lambda l} \big) \\ -\sigma^*_{\lambda P\, K}(x,y,\omega)\Delta u^k_{P,l}(y,\omega) \big] \, n_\lambda^k(y) \, d\Gamma_k \ , \quad x \in \Gamma_k \end{aligned} \tag{13}$$

Eqs.(13) forms, strictly speaking, a system of integro-differential equations with respect to the unknown Δu_J^k along the cracks.

The numerical treatment of (13) follows the procedure developed by Gross *et* al. [25] and Dineva *et* al. [26] which has been realized within a FORTRAN code. The BIEs are collocated along each crack where the displacement and traction are approximated with parabolic shape functions which satisfy H?lder continuity at least at the collocation points. Their asymptotic displacement behaviour near the crack tip is of the type $O\left(\sqrt{r}\right)$ while the traction behaves as $O\left(1/\sqrt{r}\right)$. Quarter-point boundary elements (QP-BE) are implemented in a quadratic boundary element discretization. The disadvantages of the standard quadratic approximation concerning the smoothness at irregular points as crack-tips and odd nodes of the discretization mesh are avoided by the shifted point method proposed by Rangelov *et* al. [29].

After discretization the obtained integrals are at least Cauchy principal value (CPV) integrals. The regular integrals are computed employing the Gaussian quadrature scheme for one-dimensional integrals and Monte Carlo integration scheme for two-dimensional integrals where integration is done over the boundary element and over the unit circumference which is involved in the 2D fundamental solution, see Gross *et* al. [25]. All singular integrals and integrals with logarithmic singularity are solved analytically for the small neighbourhood of the source point, using the approximation of the fundamental solution for a small argument, and numerically for the remaining part of the boundary element. Finally, satisfying the boundary conditions, an algebraic system of equations for the discrete CODs Δu_J^k, along the N cracks is obtained. Once having calculated the solution for a given frequency ω, the displacements and tractions of the scattered wave field, and by this the total field, can be determined in the whole domain from the representation formula (12).

Knowing tractions, the generalized dynamic SIFs at the tips of the $k-th$ crack are calculated by using the formulae

$$K_I^k = \lim_{\varsigma_1^k \to \mp a^k} t_3^k \sqrt{2\pi(\varsigma_1^k \pm a^k)}, \quad K_{II}^k = \lim_{\varsigma_1^k \to \mp a^k} t_1^k \sqrt{2\pi(\varsigma_1^k \pm a^k)},$$

$$K_{IV}^k = \lim_{\varsigma_1^k \to \mp a^k} t_4^k \sqrt{2\pi(\varsigma_1^k \pm a^k)} \tag{14}$$

where t_J^k, $J = 1, 3, 4$ is the generalized traction ahead of the crack-tips of the $k-th$ crack. Regarding the electrical SIFs, the electric field SIF K_E^k with $K_E^k = \lim_{\varsigma_1^k \to \mp a^k} E_3^k \sqrt{2\pi(\varsigma_1^k \pm a^k)}$ and $E_3^k = (c_{33} t_4^k - e_{33} t_3^k)(e_{33} c_{33} + e_{33}^2)^{-1}$ or the electric displacement SIF K_D^k with $K_D^k = K_{IV}^k$ can be determined. In all calculations an appropriate normalization has been used which for the mechanical SIFs is given by

$$\bar{K}_{I,II}^k = K_{I,II}^k / m \quad with \quad m = \left|\bar{t}_3^{in}\right| \sqrt{\pi a} = \omega \sqrt{\left(c_{33} + e_{33}^2 \varepsilon_{33}^{-1}\right) \rho} \sqrt{\pi a} \tag{15}$$

and where $\bar{t}_3^{in}$ is the mechanical traction of the normal incident wave. The normalized electrical SIFs are defined as $\bar{K}_E^k = e_{33}m^{-1}\left|K_E^k\right|$ and $\bar{K}_D^k = c_{33}e_{33}m^{-1}\left|K_D^k\right|$ while the normalized frequency is introduced through $\Omega = \frac{a\omega}{C_T} = a\omega\sqrt{\rho c_{44}^{-1}}$.

4 Results

4.1 Piezoelectric solids

In the following SIF results are presented for a single crack and for different two-crack configurations, see Fig.2. For simplicity all cracks are of length $2a = 5mm$. Numerical studies showed that 7 boundary elements for each crack are sufficient to achieve a satisfying accuracy within the considered frequency range. The first and the last element are QP-BE while the remaining elements

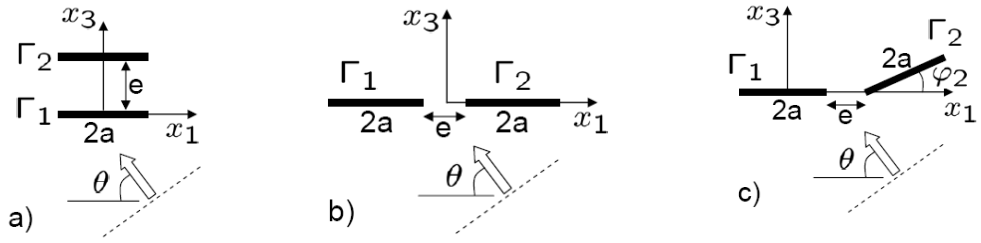

Figure 2: Two-crack systems: a) stacked cracks; b) collinear cracks; c) inclined cracks

are ordinary quadratic elements. Their lengths have been chosen as $l_1 = l_7 = 0.375mm$, $l_2 = l_6 = 0.5mm$, $l_3 = l_5 = 1.0mm$, $l_4 = 1.25mm$. Two different piezoelectric materials have been considered to make comparisons with results from the literature possible. The first one is PZT-6B with the density $\rho = 7.55 \times 10^3 kg/m^3$, elastic stiffnesses in $[10^{10}N/m^2]$: $c_{11} = 16.8$, $c_{33} = 16.3$, $c_{44} = 2.71$, $c_{13} = 6.0$, piezoelectric coefficients in $[C/m^2]$: $e_{31} = -0.9$, $e_{33} = 7.1$, $e_{15} = 4.6$ and dielectric constants in $[10^{-10}C/Vm]$: $\varepsilon_{11} = 36$, $\varepsilon_{33} = 34$. The second material is PZT-5H with the density $\rho = 7.6 \times 10^3 kg/m^3$, elastic stiffnesses in $[10^{10}N/m^2]$: $c_{11} = 12.6$, $c_{33} = 11.7$, $c_{44} = 2.30$, $c_{13} = 8.41$, piezoelectric coefficients in $[C/m^2]$: $e_{31} = -6.5$, $e_{33} = 23.30$, $e_{15} = 17.44$ and dielectric constants in $[10^{-10}C/Vm]$: $\varepsilon_{11} = 150.30$, $\varepsilon_{33} = 130$. Figure

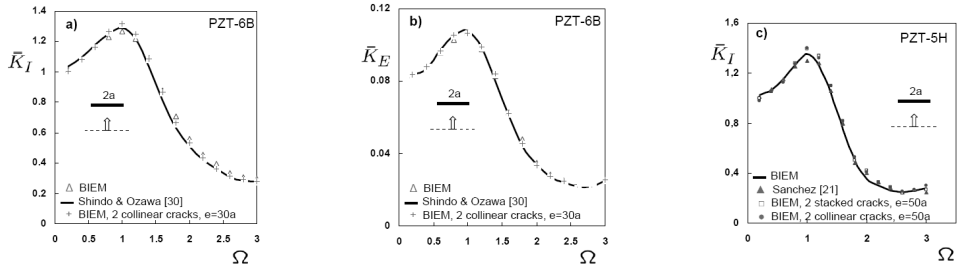

Figure 3: K-factors vs. frequency for a single crack in a piezoelectric material; comparison with results of other authors and with two-crack systems

3 shows as a test example SIF-results, here denoted as BIEM, for a single crack under normal incident L-waves which have already been presented by the authors in [25]. A comparison with those of Shindo and Ozawa [30] and Sanchez [21] leads to computational differences less than 8%. This indicates that the numerical scheme works satisfactory albeit the low number of chosen elements. The results are additionally compared with those of collinear and stacked cracks, respectively, which are far away from each of other. For this case SIFs as for a single crack can be expected since the interaction between the two cracks is neglegible on account of their large distance. This fact is properly reflected by the results which verify again the applicability of the numerical scheme. Finally, by comparison of Figures 3a and 3c, it can be observed that the shape of the SIF versus frequency curves is slightly different, i.e. the specific material properties have a noticeable influence. In Figure 4

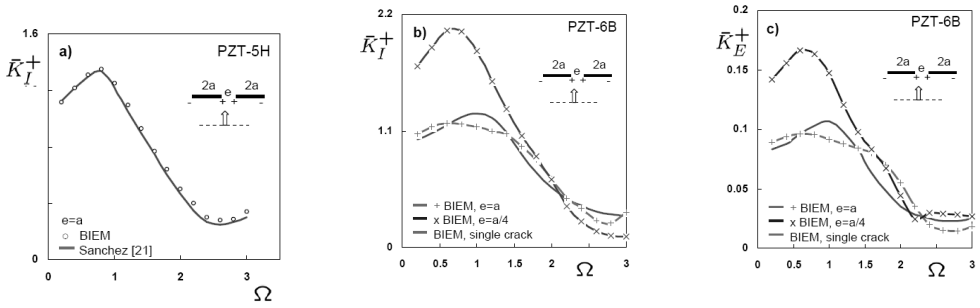

Figure 4: K-factors vs. frequency for two collinear cracks in a piezoelectric material; comparison with results of Sanchez [21] and dependence on distance e

dynamic SIFs for the inner crack tips of two collinear cracks under a normal incident L-wave are depicted. First, a comparison of our $\bar{K}_I^+$ - results with those of Sanchez [21] for the crack-tip distance e=a in Fig.4a shows again an excellent agreement. Secondly, a significant influence of the the material properties and the crack distance is noticable. For e=a the so-called dynamic overshoot, i.e. the maximum of $\bar{K}_I^+$ and its location, is different for PZT-5H and PZT-6B (Figs.4a, b). Unexpectedly, for PZT-6B this maximum is below that for a single crack wich also appears for the electric SIF. When the crack-tips approach each other the maximum SIFs in general increase. This clearly can be seen in Figs.4b,c for $e = a/4$. Stress intensity factors versus frequency

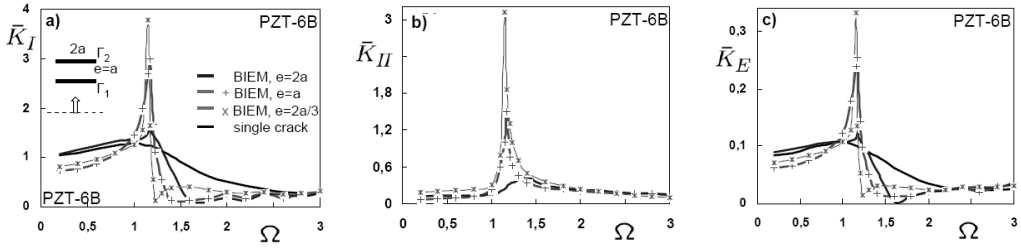

Figure 5: K-factors at crack Γ_1 vs. frequency for two stacked cracks in a piezoelectric material; dependence on distance e

for the lower crack of two stacked cracks under normal incident L-waves are plotted in Figure 5. Because this problem is unsymmetric with respect to the wave-cracks-configuration, a mode-II SIF appears. The dynamic overshoot for all SIFs of this configuration increases significantly with decreasing crack distance e. For the small crack distance $e = 2a/3$ a sharp resonance peak at $\Omega = 1.1$ can be observed, but in general the strength of the crack interaction depends on the frequency. Comparing the peak values with those for collinear cracks in Fig.4 it can be concluded that the crack interaction effect is much stronger for stacked cracks than for collinear cracks. Calculations with similar results have been done by Sanchez [21] for another material. They are not shown here because of the different material parameters. The influence of an oblique wave incidence is shown for collinear cracks in Fig.6. Considered are SIFs at the inner crack tip of the left crack for L- and SV waves with an incidence angle $\theta = \pi/4$. By comparison of Fig.6a with Fig.4b for a L-wave it can be seen that the mode-I SIFs for all crack distances e are significantly smaller than for a normal incident angle. But now in addition a mode-II SIF appears, see Fig.6b, which is not present for normal incidence. The mode-I SIFs for the SV-wave in Fig.6c are smaller than for the L-wave but they show

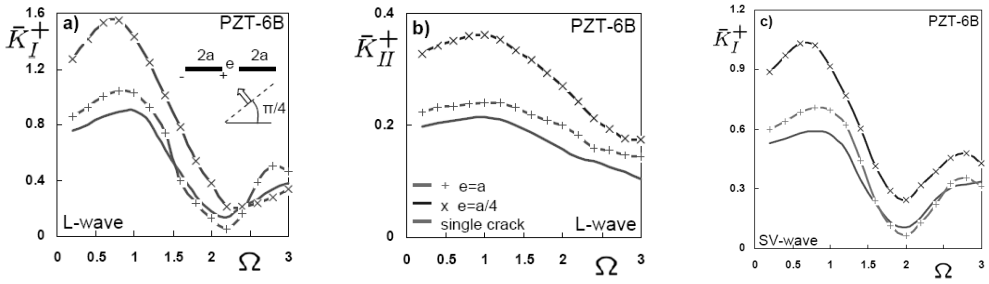

Figure 6: Collinear cracks in a piezoelectric material under oblique L- and SV-wave loading

similar dependencies on the frequency and the crack distance. Finally, the

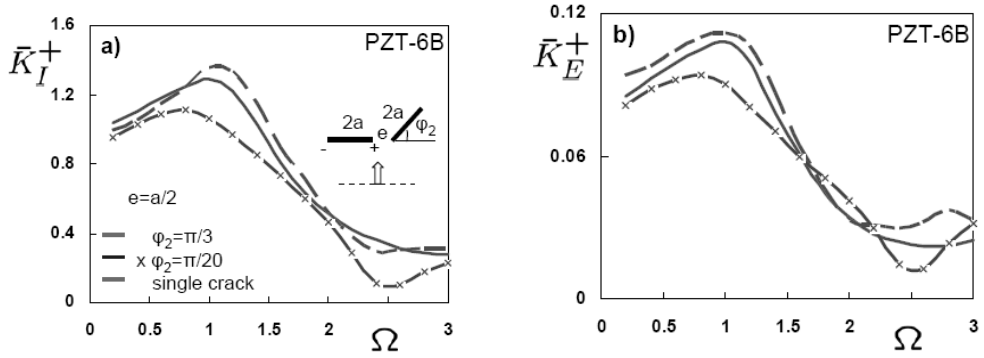

Figure 7: Two inclined cracks in a piezoelectric material under L-wave loading

influence of inclined 2^{nd} crack on the SIFs of a 1^{st} crack loaded by normal incident L-waves is shown in Fig.7 for two different inclination angles and the crack tip distance $e = a/2$. For the higher inclination angle $\varphi_2 = \pi/3$ the interaction leads to higher peak values of both the mode-I and the electric SIF compared with the results of a single crack. For the smaller inclination angle $\varphi_2 = \pi/20$ the opposite is visible, i.e. through interaction with the 2^{nd} crack the 1^{st} crack is shielded in the frequency region of the peak. On account of the unsymmetry of the configuration again a mode-II SIF is present which is not shown here.

4.2 Anisotropic solids

The following examples, for simplicity, are restricted to cracks in orthotropic materials with a symmetry axis parallel to x_3, i.e. the effect of material alignment is not considered. The investigation and the numerical scheme follow exactly the line described in sections 2-3. A detailed validation study for a single crack in an isotropic, orthotropic and transversely-isotropic material subjected to normal incident L-waves has already been given by Dineva *et* al. [26], comparing the authors' BIEM results with those of Ohyoshi [31] and Dhawan [32]. Regarding two-crack systems, without showing it in detail, the SIF-results of our numerical scheme for large distances between two interacting cracks converge, as in the piezoelectric case, to the solutions of a single crack. In Figures 8 and 9 SIFs determined by the proposed BIEM

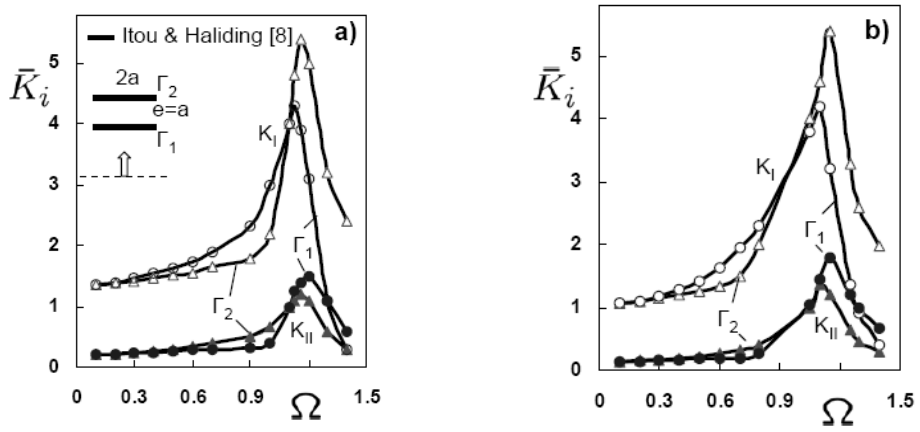

Figure 8: Two stacked cracks in an orthotropic medium under L-wave loading: a) Boron-Epoxy, b) Graphite-Epoxy

are compared with those of Itou and Haliding [8] for stacked cracks and of Itou [7] for collinear cracks under normal incident L-wave loading. The orthotropic material in Figures 8a and 9a,b is a Boron-Epoxy composite with the properties $E_1 = 224.06GPa$; $E_3 = 12.69GPa$; $\mu_{13} = 4.43GPa$; $\nu_{13} = 0.256$, while a Graphite-Epoxy composite is considered in Fig.8b with $E_1 = 158.06GPa$; $E_3 = 15.3GPa$; $\mu_{13} = 5.52GPa$; $\nu_{13} = 0.34$. The dynamic SIFs are normalized by $\sigma_0\sqrt{a}$ in [8] and by $\sigma_0\sqrt{\pi a}$ in [7], where $\sigma_0 = c_{33}\frac{i\omega}{c_T}$ and $c_T = \sqrt{\frac{c_{44}}{\rho}}$ is the shear wave velocity. Plotted are the normalized SIFs $\overset{i}{K}$ for both cracks of the stacked crack configuration in Fig.8 and for the inner (+) and outer (-) tips of the collinear crack configuration in Fig.9 versus nor-

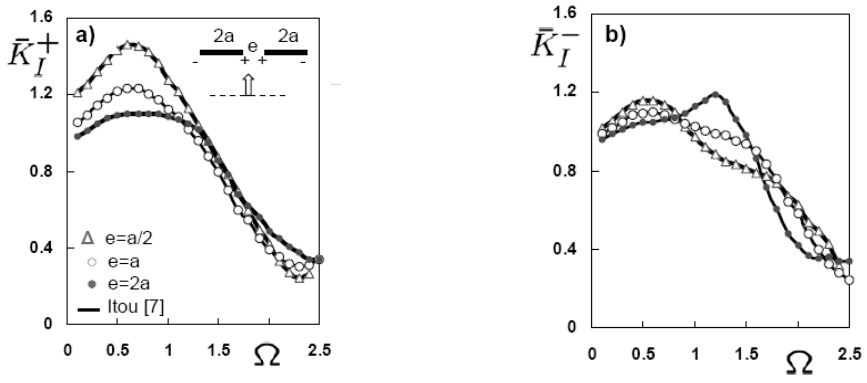

Figure 9: Two collinear cracks in an orthotropic Boron-Epoxy material under L-wave loading

malized frequency $\Omega = \frac{a\omega}{c_T} = a\omega\sqrt{\rho c_{44}^{-1}}$. Figures 8 and 9 demonstrate that the results obtained by the different computation techniques are very close. This underlines the applicability and accuracy of the proposed numerical method.

In the following we consider anisotropic materials with properties defined in [31] where $c_{ij} = s_{ij}C$ with $C = 6.6495GPa$ and $\rho = 2.4.10^3 kg/m^3$. Following the notation in [31] the so-called case-6 material is given by $s_{11} = 1,\ s_{13} = s_{31} = 1/3,\ s_{33} = 1,\ s_{44} = 1/6$ while the case-7 material has the properties $s_{11} = 1,\ s_{13} = s_{31} = 1/30,\ s_{33} = 1,\ s_{44} = 1/3$. The dynamic SIFs are now normalized by the value $\omega d_{33}^{-1/2}\sqrt{a\pi}$ where $d_{33} = \frac{c_{33}}{\rho}$ and plotted versus the normalized frequency $\Omega = \frac{a\omega}{c_L} = a\omega\sqrt{\rho c_{33}^{-1}}$ which is different from that used in Figs.8 and 9. Results for stacked cracks in a case-6 material subjected to normal incident L-waves are depicted in Fig.10. The peak values of both the mode-I and mode-II SIFs increase with decreasing crack distance. This tendency and the formation of sharp resonance peaks are similar as in the piezoelectric case, see Fig.5. Furthermore, it can be observed that compared with the single crack the peaks are shifted slightly to higher frequencies. It also should be noted that in case of a single crack no mode-II SIF is present. All these effects are clearly induced by crack interaction. The dynamic mode-I SIFs versus frequency are plotted for the inner crack tips of collinear cracks under normal incident L-wave loading in Fig.11. Compared are results for two different crack distances e and the two different materials: case-6 in Fig.11a and case-7 in Fig.11b. As expected, the peak value increases with decreasing distance e for both materials but the influence of different material parameters is significant. Mentioned in this context shall only be the differences in the

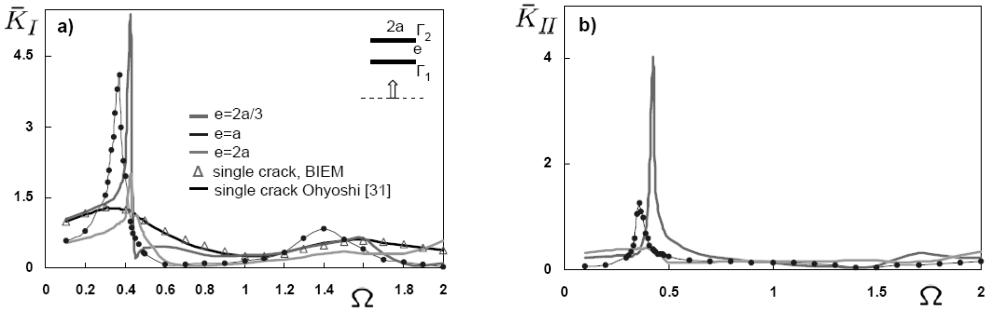

Figure 10: K-factors at crack ?1 of two stacked cracks in an orthotropic 'case-6' material under L-wave loading

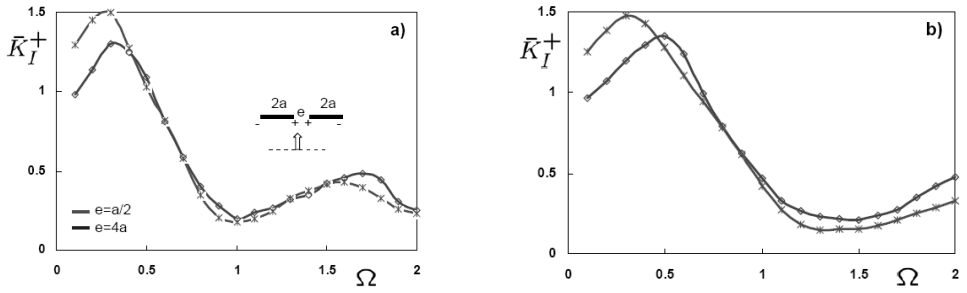

Figure 11: Two collinear cracks under L-wave loading, comparison of two different orthotropic materials: a) case-6, b) case-7

shapes of the SIF-curves, in the location of the peaks and their shift to lower frequencies for decreasing distance e. Similar phenomena can be observed in Fig.12 where again results for collinear cracks in two different materials are shown, but now for an oblique L-wave loading under $\theta = \pi/4$. Here the mode-I SIFs for the case-6 material are generally higher than for case-7 while the opposite is true for the mode-II SIFs. Fig.12c clearly reveals the frequency character of both the shielding and amplification phenomena. In the frequency interval $\Omega \in [0.1, 1]$ an amplification effect for the shortest crack distance $e = a/2$ is visible, while in the higher frequency interval $\Omega \in [1.2, 2]$ a shielding effect is present.

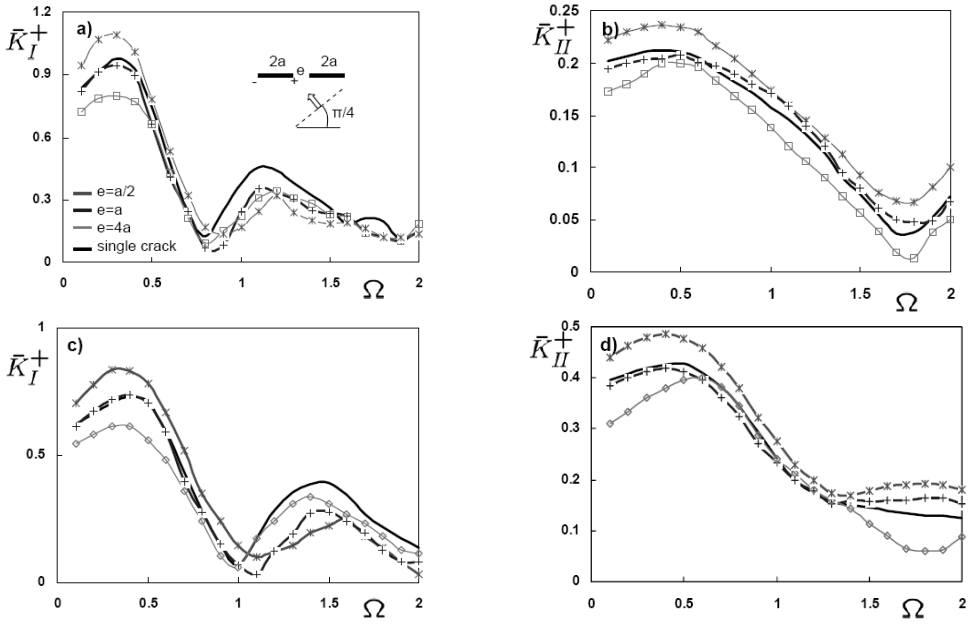

Figure 12: Two collinear cracks in an orthotropic medium under oblique L-wave loading: (a)& (b) case-6, (c)& (d) case-7

5 Conclusion

2D wave scattering by 2-crack systems of impermeable cracks in piezoelectric materials is considered. As solution procedure a numerical scheme is used which is based on nonhypersingular traction BIEM and the Radon transformed fundamental solution. Both the SIFs and the scattered wave field can be evaluated and used for application in dynamic fracture mechanics and non-destructive testing correspondingly. The elastic anisotropic problem is considered as a special case of the piezoelectric case. Numerical simulations reveal typical crack interaction phenomena such like amplification and shielding effects. Parametric studies for wave scattering by different crack systems show that the local crack tip fields, expressed by the SIFs, are a complex result of many interacting factors as the crack configuration, material properties, wave type and its characteristics, coupled character of the dynamic load and the crack-crack and wave-crack interaction phenomena.

Acknowledgements. The authors acknowledge the financial support of the DFG under the grant number 596/33-1.

References

[1] Zhou, Z., Wang, B.: The behaviour of two parallel symmetry permeable interface cracks in a piezoelectric layer bonded to two half piezoelectric materials planes. International Journal of Solids and Structures **39** 4485-4500 (2002)

[2] Sun, Y.: Multi-interface cracks in a piezoelectric layer bonded to two half-piezoelectric spaces under anti-plane shear loading. Mechanics Research Communication **30** 443-454 (2003)

[3] Zhou, Z., Wang, B., Cao, M.: The behaviour of permeable multi-cracks in a piezoelectric material. Mechanics Research Communications **30** 395-402 (2003)

[4] Gao, C., Fan, W.: A general solution for the plane problem in piezoelectric media with collinear cracks. International Journal of Engineering Science **37** 347-363 (1999)

[5] Han, J.J., Chen, Y.H.: Multiple parallel cracks interaction problem in piezoelectric ceramics. International Journal of Solids and Structures **36** 3375-3390 (1999)

[6] Zhou, Z.G., Wu, L.Z.: Basic solutions of two parallel mode-I cracks or four parallel mode-I cracks in the piezoelectric materials. Engineering Fracture Mechanics **74** 1413-1435 (2007)

[7] Itou, S.: Dynamic stress intensity factors of two collinear cracks in orthptropic medium subjected to time-harmonic disturbance. Theoretical and Applied Fracture Mechanics **25** 155-166 (1996)

[8] Itou, S., Haliding, H.: Dynamic stress intensity factors around two parallel cracks in an infinite-orthptropic plane subjected to incident harmonic stress waves. International Journal of Solids and Structures **34(9)** 1145-1165 (1997)

[9] Wang, X.D., Meguid, S.A.: Effect of electromechanical coupling on the dynamic interaction of cracks in piezoelectric materials. Acta Mechanica **143** 1-15 (2000a)

[10] Wang, X.D., Meguid, S.A.: Modelling and analysis of the dynamic behaviour of piezoelectric materials containing interacting cracks. Mechanics of Materials **32** 723-737 (2000b)

[11] Wang, X.D., Meguid, S.A.: Diffraction of SH waves by interacting matrix crack and an inhomogeneity. ASME Journal of Applied Mechanics **64** 568-575 (1997)

[12] Wang, X.D.: On the dynamic behaviour of interacting interfacial cracks in piezoelectric media. International Journal of Solids and Structures **38** 815-831 (2001)

[13] Zhao, X., Meguid, S.A.: On the dynamic behaviour of a piezoelectric laminate with multiple interfacial collinear cracks. International Journal of Solids and Structures **39** 2477-2494 (2002)

[14] Meguid, S.A., Chen, Z.T.: Transient response of a finite piezoelectric strip containing coplanar insulating cracks under electromechanical impact. Mechanics of Materials **33** 85-96 (2001)

[15] Huang, H., Shi, H., Yin, Y.: Multi-cracks problem for piezoelectric materials strip subjected to dynamic loading. Mechanics Research Communications **29** 413-424 (2002)

[16] Chen, Z.: Transient response of a piezoelectric ceramic with two coplanar cracks under electromechanical impact. Acta Mechanica Sinica **15(4)** 326-333 (1999)

[17] Chen, Z., T., Worswick, M.J.: Antiplane mechanical and inplane electric time-dependent load applied to two coplanar cracks in piezoelectric ceramic material. Theoretical and Applied Fracture Mechanics **33** 173-184 (2000)

[18] Sun, J.L., Zhou, Z.G., Wang, B.: Dynamic behaviour of uneaqual parallel permeable interface multi-cracks in a piezoelectric layer bonded to two piezoelectric materials half planes. European Journal of Mechanics A/Solids **23** 993-1005 (2004)

[19] Li, X.F., Lee, K.Y.: Dynamic behaviour of a piezoelectric ceramic layer with two surface cracks. International Journal of Solids and Structures **41** 3193-3209 (2004)

[20] Su, R.K.L., Wemjie, F., Jinxi, L., Zhenzhu, Z.: Transient response of coplanar interfacial cracks between two dissimilar piezoelectric strips under anti-plane mechanical and in-plane electrical impacts. Acta Mechanica Solida Sinica **16(4)** 300-312 (2003)

[21] Sanchez, F.G.: Numerical study of fracture problems in elastic anisotropic and piezoeleztric solids. PhD Thesis, Engineering High School, University of Sevilla, Spain (2005)

[22] Sanchez, F.G., Saez, A., Dominguez, J.: Two-dimensional time-harmonic BEM for cracked anisotropic solids. Engineering Analysis with Boundary Elements **30** 88-89 (2006)

[23] Saez, A., Sanchez, F.G., Dominguez, J.: Hypersingular BEM for dynamic fracture in 2-D piezoelectric solids. Computer methods in applied mechanics and engineering **196** 235-246 (2006)

[24] Zhang, C.H., Gross, D.: On wave propagation in elastic solids with cracks.Computational Mechanics Publication, Southampton (1998)

[25] Gross, D., Rangelov, T., Dineva, P.: 2D Wave scattering by a crack in a piezoelectric plane using traction BIEM. Journal of Structural Integrity & Durability **1(1)** 35-47 (2005)

[26] Dineva, P., Gross, D., Rangelov, T.: Wave scattering in cracked piezoelectric materials-A BIEM Approach. Journal of Theoretical and Applied Mechanics **36 (2)** 65-88 (2006)

[27] Davi, G., Milazzo, A.: Multidomain boundary integral formulations for piezoelectric materials fracture mechanics. International Journal of Solids and Structures **38** 7065-7078 (2001)

[28] Gross, D., Zhang, C.H.: Diffraction of SH waves by a system of cracks: solution by an integral equation method. International Journal of Solids and Structures **24(1)** 41-49 (1988)

[29] Rangelov, T., Dineva, P., Gross, D.: A hyper-singular traction BIEM for stress intensity factor computation in a finite cracked body. Engineering Analysis with Boundary Elements **27** 9-21 (2003)

[30] Shindo, Y., Ozawa, E.: Dynamic analysis of a cracked piezoelectric material. In: Hsieh, RKT, edd. Mechanical Modeling of New Electromagnetic materials. Elsevier, 297-304 (1990)

[31] Ohyoshi, T.: Effect of orthotropy on singular stresses for a finite crack. ASME Journal of Applied Mechanics **40** 491-497 (1973)

[32] Dhawan, G.K.: Interaction of elastic waves by a Griffith crack in an infinite transversely – isotropic medium. International Journal of Fracture **19** 29-37 (1982)

Submitted on February 2008.

Dinamička interakcija prslina u piezoelektričnim i anizotropnim čvrstim telima: a nehipersingularni BIEM pristup

U radu se predlaže nehipersigularan metod graničnih elemenata za analizu sistema prslina u piezoelektričnom anizotropnom materijalu izloženom harmonijskom talasu. Metod je baziran na fundamentalnom rešenju dobijenom Radonovom transformacijom zavisnom od frekvencije. Predloženi metod je fleksibilan, numerički efikasan i bez ograničenja u pogledu primene na materijale, geometriju prsline i tip talasa.

Tačnost metode graničnih elemenata za odredjivanje faktora intenziteta napona je proverena sa postojećim rezultatima u literaturi. U radu se simuliraju i diskutuju različite konfiguracije prslina ka što su ravanske, kolinearne ili prsline u proizvoljnom položaju jedne prema drugoj. Sve simulacije pokazuju izuzetan efekat elektromehaničke spregnutosti, kao i pojavu prigušenja odnosno pojačavanja u zavisnosti od frekvencije kao i zavisnost K faktora od kompleksnog uticaja interakcije talasa i prsline kao i interakcije izmedju samih prslina.

doi:10.2298/TAM0801073D Math.Subj.Class.: 74L15, 92C37